JACS
JOURNAL OF THE AMERICAN CHEMICAL SOCIETY
pubs.acs.org/JACS
Article

Beyond Thiol-Enzyme Inhibition: Sterically Bulky NHC-Au(I) Complexes are Catalytically Active Anticancer Agents with Reprogrammed Immunomodulatory Function

Zhi Zhong,[‡] Haitao Liu,[‡] Qiong Wu,[‡] Bei Cao,[‡] Yujiao Peng, Moyi Liu, Liang-Mei Yang, Yue Lin, Ke-Bin Huang,* Xiaolin Xiong,* Jinsai Shang,* and Taotao Zou*

Cite This: https://doi.org/10.1021/jacs.5c19777

Read Online

ACCESS | Metrics & More | Article Recommendations | Supporting Information

ABSTRACT: Metallodrug-induced immunogenicity offers significant potential for improving the efficacy of cancer immunotherapy with metals such as gold serving as a notable example. However, heavy metals may concurrently disrupt immune cell function, and a few of them can augment immunogenicity without compromising immunological integrity. Here, we report sterically bulky Au(I) complexes as catalytically active anticancer agents with the capability to reprogram immunomodulatory function. Our initial studies identified complex IPr−Au-Cl, characterized by bulky substituents, which catalytically activated an alkyne probe in the presence of GSH and triggered hydride transfer from NADH to NAD^+. Subsequent structural optimization led to the development of **Au-8**, which showed an increased catalytic activity and improved cytotoxicity against cancer cells. Although **Au-8** induced elevated ROS levels and immunogenic CRT exposure in cancer cells akin to auranofin, it triggered unique proteomic responses, notably showing minimal inhibition of thioredoxin reductase 1 (TrxR1), a crucial protein for maintaining immune cell function. Auranofin's inhibition of TrxR1 resulted in immunosuppression at one-seventh of its cytotoxic IC_{50} against cancer cells. In contrast, **Au-8** not only maintained but also enhanced immune function *in vitro*, *ex vivo*, and *in vivo*, including activated immunogenic phagocytosis and cytotoxic effects in human peripheral blood mononuclear cells isolated from healthy donors. This study, therefore, presents a novel design for gold compounds that leverages steric hindrance to achieve catalytic anticancer activity without affecting TrxR1, opening avenues for future gold-based therapeutics with desirable immunomodulatory effects.

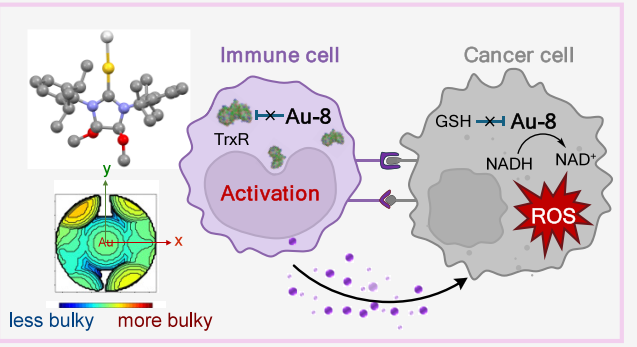

INTRODUCTION

Reactive oxygen species (ROS) play critical yet paradoxical roles in biological processes, acting as essential signaling molecules while also causing cellular damage.[1] For cancer development, ROS is beneficial to proliferation, metastasis, and accumulation of tumorigenic mutations.[2] Consequently, many cancers exhibit elevated baseline levels of ROS compared to normal tissues.[3] This altered redox homeostasis makes intracellular antioxidant defenses vital for cancer cells to prevent cytotoxic ROS accumulation.[4] Exploiting this vulnerability through pro-oxidant agents represents a promising therapeutic strategy. Notably among these targets is thioredoxin reductase 1 (TrxR1), a key enzyme governing cellular redox balance that is frequently overexpressed in malignancies and has emerged as an attractive target for anticancer drug development.[5] Indeed, analysis of *TXNRD1* gene (coding TrxR1) in human patients showed that 17 out of all tested tumor types exhibited a higher expression compared to their paired normal tissues (Scheme 1a, data from GEIPIA 2,[6] see full list in Table S1). Critically, this elevated *TXNRD1* expression correlates with poorer survival outcomes across multiple cancers.[7−9]

Due to the strong binding affinity of gold ion toward thiol and/or selenol residues,[10−24] the clinical antirheumatic drug auranofin is a classic TrxR inhibitor under global investigation for cancer therapy.[25−27] In past years, extensive endeavors have highlighted the great potential of gold(I/III) complexes in anticancer therapies,[28−45] with notable examples even inducing exceptionally long-lived immunogenic cell death (ICD) in vivo.[46−49] However, a reverse situation was observed in blood samples, where normal cells exhibited a significantly higher TrxR1 expression than cancerous ones. Noteworthily, the

Received: November 7, 2025
Revised: February 3, 2026
Accepted: February 5, 2026

Scheme 1. (a) mRNA Levels of the *TXNRD1* in Normal and Tumor Samples of Different Human Organs[a] and (b) Conceptual Scheme of Gold(I) Complexes with Large Steric Hindrance That Avoid Inhibiting TrxR Proteins and Reshape the Mode of Action Towards Cancer and Immune Cells by Catalytically Promoting ROS in Cells[b]

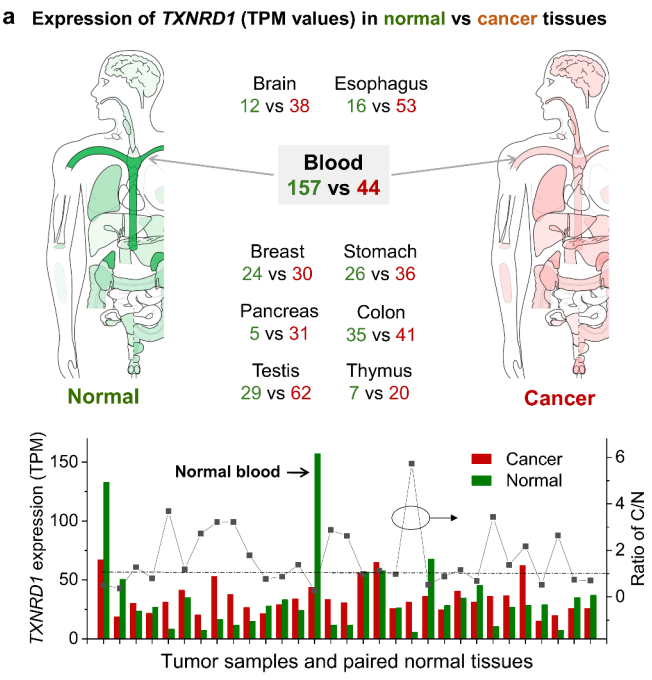

[a]The bodymap picture and expression profile were regenerated from GEPIA 2.[6] [b]Created with Biorender.com.

relative abundance of the *TXNRD1* gene (coding TrxR1) expression level, described as transcripts per million (TPM), in normal blood cells ranked among the highest (>150), exceeding stomach cancer by 4.3-fold, colorectal cancer by 3.7-fold, and pancreatic cancer by 5.1-fold (Scheme 1a and Table S1). Previous studies have pointed out the protective role of TrxR1 in the immune function of monocytes and macrophages using auranofin as the canonical inhibitor.[50−53] This protein is also essential for the expansion of activated T cells.[54] Therefore, the ROS-promoting cancer treatment targeting TrxR1 may hinder its ability to stimulate anticancer immune responses once administered systemically, despite the immunogenic potential in tumor cells.[55−59] Maintaining the capability of ROS generation while keeping TrxR1 functional is beneficial to the anticancer activity of gold complexes.[49,60−62]

Besides enzyme inhibition, gold also exhibits catalytic activities with medicinal potential.[63] A surface-clean nanocrystalline gold nanoparticle is currently being evaluated in clinical trials for rescuing the energy production of damaged neurons in patients with amyotrophic lateral sclerosis, multiple sclerosis, or Parkinson's disease.[64,65] On the other hand, soluble gold complexes display remarkable activity in homogeneous catalysis, including redox reactions potentially useful for modulating ROS production.[66,67] However, their cellular catalytic activities can seldom be maintained due to strong quenching by biological thiols, especially millimolar concentrations of glutathione (GSH).[68−70]

In view that the Cys residue in GSH is hindered by Gly and Glu,[71−74] we conceived that sterically bulky gold complexes could resist GSH binding, and this resistance should prevent TrxR inhibition while preserving catalytic access to specific biological substrates (Scheme 1b).[75−79] In this work, we evaluated the catalytic anticancer activities of gold complexes beginning with NHC-Au(I)-Cl due to its easily tunable NHC ligand and remarkable catalytic/bioactive properties.[19,80−90] Notably, sterically hindered complexes such as IPr-Au(I)-Cl (IPr = 1,3-bis(2,6-diisopropylphenyl)imidazol-2-ylidene; **Au-3**), maintained catalytic activity in the presence of GSH while efficiently triggering NADH-to-NAD$^+$ conversion. Subsequent ligand optimization yielded **Au-8**, which exhibited enhanced catalytic activity and superior anticancer efficacy against human colorectal HCT116 cells. Importantly, while **Au-8** shows ROS-promoting and calreticulin-exposing behaviors in cancer cells similar to auranofin, it does not inhibit TrxR1. This divergence reprograms immunomodulatory functions typically associated with auranofin while potentiating immune activation at noncytotoxic concentrations of **Au-8**. To the best of our knowledge, this represents the first demonstration of catalytically active gold anticancer complexes that enable reprogrammed immunomodulatory function.

RESULTS AND DISCUSSION

Preparation of Gold Complexes and Evaluation of Catalytic Activity in the Presence of GSH

First, we collected seven potentially catalytic-active Au(I)/Au(III) complexes **Au-1** to **Au-7** (Figure 1a) either from commercial source or preparation following the literature procedure.[91,92] These complexes are highly soluble in organic solvents such as CH_2Cl_2, DMSO, DMF, and CH_3CN. Typically, these gold complexes were prepared as 10 mM stock solutions in DMSO and then diluted with an aqueous solution for subsequent experiments.

As mentioned in the literature, the Au−Cl bond could undergo hydrolysis in aqueous solution,[93−95] which is critical for their catalytic activities in aqueous solution.[9,69] Taking NHC-Au-Cl type of complexes as an example, after dissolving the compound in aqueous solution containing different organic solvents, we detected NHC-Au-DMSO and NHC-Au-CH_3CN, with m/z = 371.0492, and 334.0618, respectively, in the case of **Au-1** (Figure S1a), and IPr-Au-DMF with m/z = 658.3074 for **Au-3** (Figure S1b), supporting the possibility of Au−Cl breakage in aqueous solution.

https://doi.org/10.1021/jacs.5c19777
J. Am. Chem. Soc. XXXX, XXX, XXX−XXX

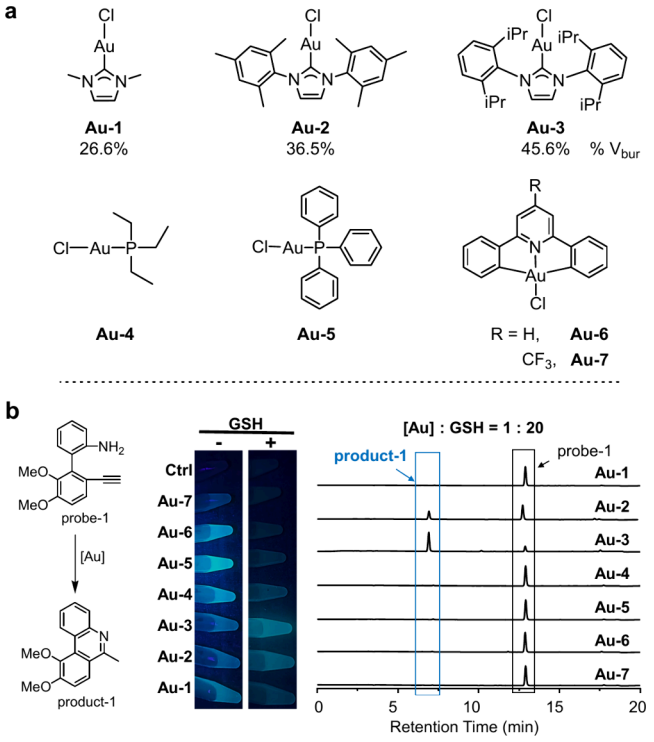

Figure 1. (a) Chemical structures of gold complexes **Au-1** to **Au-7** in this study. The buried volume (% V_{bur}) of gold by the cognate NHC ligand was calculated based on SambVca 2.1.[96] (b) Left: The synthesized probe-1 for measuring the intramolecular cyclization reaction catalyzed by gold compounds. Middle: Images under 365 nm UV light of reaction mixture after 24 h of incubation at 37 °C. Right: HPLC chromatogram of the reaction mixture. GSH (4 mM) was in 20-fold molar excess to gold catalysts.

Then, we screened their catalytic activities in aqueous solution. An alkyne-based probe-1 (2′-ethynyl-[1,1′-biphenyl]-2-amine derivative) was employed since it can be converted into fluorescent phenanthridine-derived product-1 via hydroamination reaction by active gold catalysts (Figure 1b).[97] After incubating 1 mM probe-1 and 200 μM indicated gold compounds in water (containing 50% CH_3CN, v/v), we immediately observed fluorescence in **Au-1** to **Au-6**, with **Au-5** showing the highest emission intensity (Figure S2). However, the addition of 4 mM GSH (20-fold excess to gold) to the reaction mixture significantly suppressed the catalytic activities of these complexes. Despite this, after 24 h of incubation at 37 °C, **Au-2** (IMes-Au-Cl, IMes = 1,3-bis(2,4,6-trimethylphenyl) imidazol-2-ylidene) and **Au-3** still maintained the fluorescence intensity (Figure 1b, middle). HPLC analysis showed that **Au-2** and **Au-3** triggered 46.6% and 83.8% conversion, respectively, when GSH was coincubated (Figure 1b, right). In the literature, it is known that the Au−C_{NHC} bond is stronger than Au−P to resist thiol attack, leading to no/weak fluorescence intensity and hence low catalytic activity for **Au-4** and **Au-5**. In the type of NHC-Au-Cl, the buried volume (% V_{bur}), which is defined as the percentage of a sphere (r = 3.5 Å) around the gold ion occupied by the ligand,[96] increased from **Au-1** (26.6%) to **Au-2** (36.5%) and **Au-3** (45.6%). Thus, the steric hindrance in NHC could help to prevent the interaction of GSH from binding to active gold, while preserving catalytic activities.

Au-3-Induced NADH-to-NAD$^+$ Conversion

The above-mentioned catalytic hydroamination reaction suggests IPr-Au$^+$ displays π acidity, a form of Lewis acidity that allows metal centers to accept Lewis bases.[98] Since IPr-Au$^+$ is known to stabilize the hydride intermediate,[99] we examined whether the endogenous NADH can serve as a hydride donor. After incubating **Au-3** (20 μM) with 5-fold NADH in an aqueous solution (H_2O/DMSO, 1:1, v/v) at 37 °C, UV−vis absorption analysis showed a time-dependent decrease of absorbance at 320−400 nm, with an isosbestic point at 307 nm (Figure 2a, b), which is typical of NADH-to-

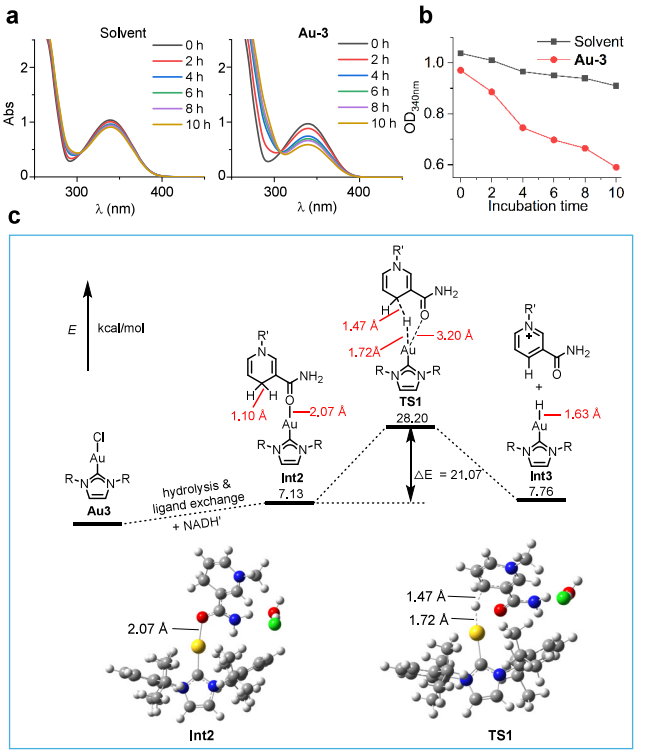

Figure 2. Complex **Au-3** triggers NADH-to-NAD$^+$ conversion. (a) UV−vis absorption spectra for the mixtures of 20 μM **Au-3** with 100 μM NADH in H_2O/DMSO (1/1, v/v) at 37 °C after different incubation periods. (b) Plot of OD_{340nm} versus incubation time for the UV−vis absorption spectra as shown in (a). (c) DFT calculations for the energy barriers of the hydride transfer process.

NAD$^+$ oxidation.[100−102] Further quantification of NADH was performed by using a colorimetric assay based on WST-8, a dye that reacts with NADH to produce a yellow color measured at OD_{450nm}. The results indicated a conversion of ~50% after 6 h of incubation (Figure S3a,b). This indicates that the process is catalytic despite the low turnover number observed during this incubation period. Formation of NAD$^+$ was further confirmed by adding alcohol dehydrogenase, which specifically converts NAD$^+$ back to NADH, resulting in a further increased absorbance after addition of WST-8 (Figure S3c). Notably, even in the presence of GSH, **Au-3** still maintained activity for triggering NADH-to-NAD$^+$ conversion (Figure S4). Then, we replaced H_2O in the reaction solvent with saline (0.9% w/v NaCl in water) to better simulate the physiological condition. We noted that **Au-3** exhibited poor solubility in a saline and DMSO mixture (1/1, v/v), but additionally adding the solubilizer F127 could enhance the

https://doi.org/10.1021/jacs.5c19777
J. Am. Chem. Soc. XXXX, XXX, XXX−XXX

solubility of **Au-3** and regain its activity to convert NADH to NAD^+ (Figure S5).

To achieve insights into the mechanism of hydride transfer, density functional theory (DFT) calculations were performed. Initial attempts to capture the direct intermediate of hydride to the Au−Cl transfer adduct resulted in a high energy barrier of +39.26 kcal/mol, which is unfavorable for the reaction (Figure S6). However, if the Cl ligand is hydrolyzed, it will then favor a weak coordination of the carbonyl of NADH to the Au ion, forming **Int2** (note that a possible carbonyl to Au coordination adduct, IPr-Au-DMF was captured by HRMS, Figure S1b). This leads to a facile hydride transfer to Au (via **TS1**) with a favorable energy barrier of +21.07 kcal/mol, subsequently generating IPr-Au-H (**Int3**) with a comparable energy to **Int2** (Figure 2c). This IPr-Au-H species is known to be unstable[99] and may further react with molecular oxygen to form multifaceted peroxide species.[103−105]

Development of an Analogous Au-8 with Potent Anticancer Activities

Despite the potential of NADH-to-NAD^+ oxidation to disrupt cellular redox homeostasis and kill cancer cells,[106−113] the cytotoxicity of **Au-3** is moderate (Figure S7),[114] likely due to its low water solubility, which hampers hydrolysis of Cl ligand and its cellular bioavailability. To address this, we tried to modify **Au-3** by retaining the IPr ligand scaffold while replacing the auxiliary ligand by reacting with silver salts containing weak donating anions such as NTf_2^- [bis-(trifluoromethylsulfonyl)amide, OTf^- (trifluoro-methanesulfonate), and TFA^- (trifluoroacetate). These modifications resulted in improved water solubility and enhanced cytotoxicity, especially in the case of TFA as an anion (Figure S7). Afterward, we modified the IPr ligand by keeping the bulky 1,3-bis(2,6-diisopropylphenyl) groups while modifying the imidazole moiety, and finally, we obtained **Au-8** containing a 4,5-dimethoxy-4,5-dihydroimidazol-2-ylidene moiety. This compound shows a similar steric hindrance ($\%V_{burr}$ = 45.5%, Figure 3a) based on its crystal structure of the Cl analogue (Figure 3a and Table S2). Of note, the two out-of-plane methoxy groups additionally introduce steric rigidity. When the dihedral angle between the phenyl plane and N-heterocyclic ring is changed (C−N−C−C), the energy barriers of **Au-8**, as calculated by DFT, are much higher than that of **Au-3** (Figure 3a). In an aqueous solution, **Au-8** triggered the cyclization of probe-1 (Figure S8) and NADH-to-NAD+ (Figure S9) conversion in a similar efficiency to **Au-3** either with or without GSH. Of note, when incubating the mixture of **Au-8** with 2 equiv of NADH in an aqueous solution (CH_3CN/H_2O, 1/1 v/v) for 16 h, we successfully detected a signal with an m/z of 671.2892 by HRMS (Figure 3b). The mass and isotopic pattern of this signal correspond to the formation of $[NHC−Au-H + Na]^+$.

While **Au-3** and **Au-8** demonstrated similar catalytic activity in aqueous solutions, **Au-8** retained its catalytic effectiveness under cellular-like conditions—such as incubation with concentrated, freshly prepared HCT116 cell lysates—by successfully triggering the cyclization of probe-1. In contrast, **Au-3** exhibited minimal activity (Figure 3c, i). Moreover, if the living HCT116 cells were treated with **Au-8** for 0.5 h followed by removing the medium and washing, and then adding probe-1 for another 0.5 h incubation, clear emission can be found (Figure 3c, ii). However, under similar conditions using **Au-3**, no obvious fluorescence can be observed. These results

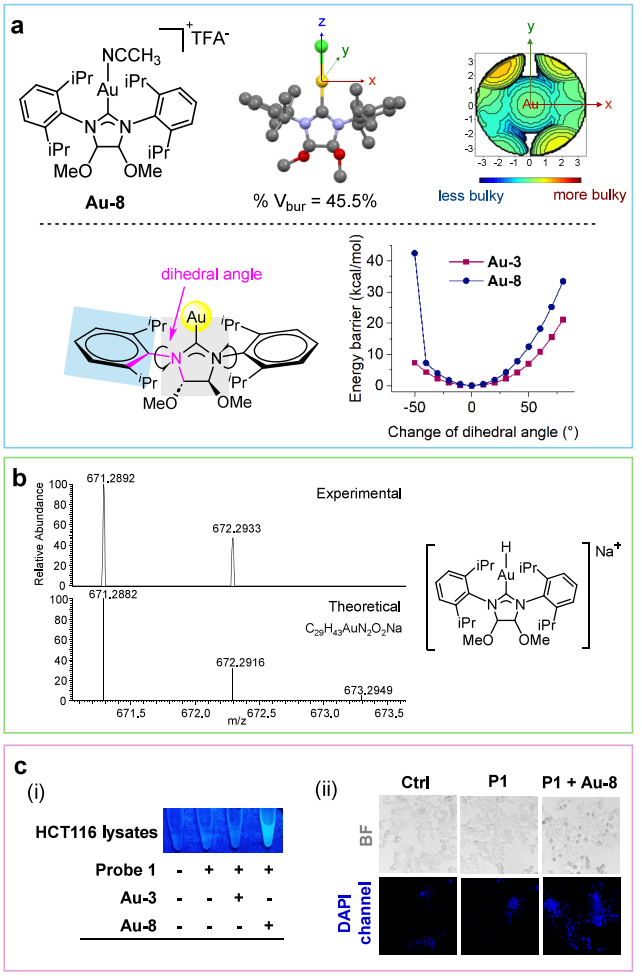

Figure 3. Development of an analogous **Au-8**. (a) Upper left: the chemical structure of **Au-8** (note: the coordinated solvent may vary depending on the preparation/purification condition); middle: the crystal structure of the Cl analog of **Au-8** (CCDC 2421111, Table S2); upper right: the topographic steric map of the ligand. Lower panel: the energy barriers when changing the dihedral angle by rotating the phenyl plane of **Au-3** and **Au-8**. (b) HRMS analysis for the mixture of **Au-8** with 2 equiv of NADH in an aqueous solution (CH_3CN/H_2O, 1/1 v/v) for 16 h. (c) Monitoring the catalytic activity of **Au-8** in the HCT116 cell lysates by adding 50 μM of gold compounds and 100 μM of probe-1 in cell lysate for 24 h (i). Examination of the cellular catalytic of **Au-8** was carried out by treating HCT116 cells with **Au-8** for 0.5 h, followed by washing the medium thrice before adding probe-1 for another 0.5 h incubation. The images were taken under a DAPI fluorescence channel (ii).

indicate that **Au-8** has a greater number of cellular catalytic activities. Consequently, **Au-8** exhibited enhanced cytotoxicity, with an IC_{50} of 4.67 ± 0.61 μM against HCT116 cells (note that TFA anion display no cytotoxicity with IC_{50} > 1 mM for NaTFA), making it five times more potent than **Au-3** (Figure S7). Such a cytotoxicity is only slightly lower than that of auranofin (IC_{50} = 2.90 ± 0.36 μM). However, after treating HCT116 cells with **Au-8** or auranofin for 5 h, the gold content in the **Au-8** treatment group is <5% compared to the auranofin group (Figure S10), suggesting a much more efficient cell-killing mechanism that is different from auranofin.[115,116]

To elaborate the anticancer mode-of-action, we monitored the proteomic responses of HCT116 cells after 24 h of incubation with 5 μM **Au-8** (Figure 4a, i). The results showed

https://doi.org/10.1021/jacs.5c19777
J. Am. Chem. Soc. XXXX, XXX, XXX−XXX

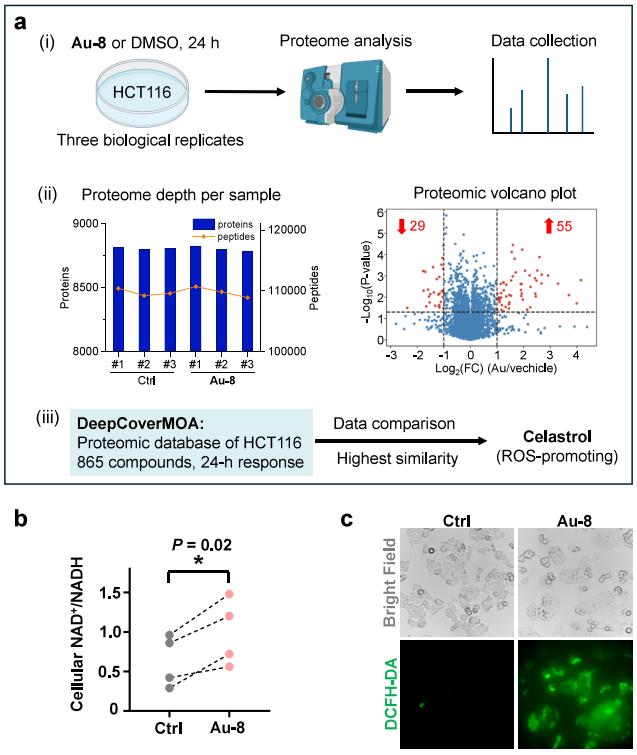

Figure 4. Au-8 as a potent pro-oxidant. (a) Proteomic study for HCT116 cells treated by **Au-8** for 24 h. (i) Experimental procedure, (ii) detected proteins/peptides per sample (left), and the volcano plot of the proteomic data (right). (iii) Comparative analysis of **Au-8** with other anticancer agents using a web server DeepCoverMOA identifies celastrol with the highest similarity. (b) The cellular ratio of NAD^+/NADH after HCT116 cells treating with **Au-8** (5.0 μM) for 6 h. (c) Fluorescence images of HCT116 cells after treatment by **Au-8** (5.0 μM) for 6 h and stained with DCFH-DA.

a high proteome depth with over 8,500 proteins and >110,000 peptides detected in each sample (Figure 4a, ii, left). There were 55 proteins significantly upregulated, and 29 proteins downregulated compared to the control group (Figure 4a, ii, right). The altered proteins are centered by two transcriptional regulators, Jun and ATF3 (Figure S11). These regulators have been linked to cellular stresses such as ER (endoplasmic reticulum) stress[117] and oxidative stress.[118] Next, we compared the proteome changes of the treated HCT116 cells with known anticancer agents using the DeepCoverMOA server.[119] This recently developed database collected the 24-h proteomic responses of HCT116 cells toward more than 800 anticancer compounds. The comparative analysis unveiled the most similar hit (Pearson $r = 0.71$, positively correlated) as celastrol, a known ROS-promoting natural product (Figure 4a, iii).[120−122]

Indeed, **Au-8** displayed a high ROS-inducing capability. After treating HCT116 cells with **Au-8** for 6 h, a significant elevation in the cellular NAD^+-to-NADH ratio was observed in the cell lysates ($p < 0.05$, Figure 4b), consistent with its activity in converting NADH to NAD^+ in solution (Figure S9). This is along with a substantial accumulation of intracellular ROS, as revealed by strong green emission after staining by DCFH-DA, a fluorescent probe measuring total cellular ROS, in the treated HCT116 cells (Figure 4c). To assess the specific ROS under such treatment conditions, four probes were employed, including BES-H_2O_2-Ac for H_2O_2, aminophenyl fluorescein (APF) for HO• radicals, singlet oxygen sensor green (SOSG) for $^1O_2$ and dihydroethidium (DHE) for $O_2^{\bullet-}$. As shown in Figure S12, HCT116 cells treated with **Au-8** showed signals of H_2O_2 and HO• radicals, but not $^1O_2$ or $O_2^{\bullet-}$. Such results are consistent with formation of Au-peroxide species (Figure S13), which reinforced the catalytic mechanism: the NHC-Au species accepts a hydride from NADH, forming NAD^+ and NHC−Au-H; the Au-hydride species can then undergo O_2 insertion, generating Au-peroxide species for subsequent oxidative reactions (Figure S14).

Au-8, Unlike TrxR-Targeting Auranofin, Does Not Attenuate Immune Responses

The FDA-approved gold drug auranofin confers immunosuppressive activity in activated immune cells. It is thus used as an antirheumatic drug to suppress overactive immune systems. Unlike auranofin, **Au-8** holds a large steric hindrance to avoid attacking the thiol/selenol enzymes like TrxR1. This drives us to identify the different intracellular mechanisms of these two agents, even though both can induce oxidative stress. The human monocytic cell line THP-1 cells were treated with phorbol 12-myristate 13-acetate (PMA), a stimulus that can induce macrophage differentiation, for 24 h followed by a one-day resting in no-PMA medium. The cytotoxicity IC_{50} values of auranofin and **Au-8** to the THP-1-derived macrophages were determined to be 18.9 ± 1.2 and 28.1 ± 2.1 μM, respectively, the potencies of which are much lower than that toward cancer cells.

Then, these macrophages (Mφ) were incubated with the gold compounds for 24 h at a low concentration of 1 μM (less than one-tenth of their cytotoxicity IC_{50}). The proteomic profiling was conducted to compare cellular responses to different treatments. Results showed that auranofin induced the downregulation of key immunological proteins CD14, CD86, TGFB3, CD163, and TNF, whereas **Au-8** displayed negligible activity (Figure 5a). Of note, in the upregulated proteins, TrxR1 is one of the significantly upregulated proteins in the auranofin group (**AF**) versus the **Au-8** group. A STRING[123] map of protein−protein interactions indicates a centered role of TrxR1 in all the upregulated proteins (Figure 5a). Such a higher expression is possibly a compensatory mechanism in response to the strong inhibition of this protein by auranofin, matching the previous studies identifying TrxR1 as the primary target of auranofin.[124,125] Inspired by this, we conducted assays measuring the enzyme activities by using purified TrxR1. According to the results (Figure 5b), **Au-8** exhibited much weaker inhibitory effects than auranofin (57.3 nM versus 2.4 nM). An assay of cellular TrxR activities using the lysates of treated HCT116 cells demonstrated a similar trend (17.4 versus 1.5 μM; Figure 5b). Besides, the TrxR activity, measured by the fluorescence of a TrxR-specific TRFS-green probe[126] in living cells, was severely inhibited by auranofin but not by **Au-8** at their IC_{50} concentrations on both HCT116 cells and THP-1 macrophages (Figure 5c). These data together suggested that **Au-8** functions differently from auranofin with significantly reduced TrxR inhibition.

Next, we sought to verify whether **Au-8**, without targeting TrxR1, exhibits a different effect on immunity. In the previous work, auranofin has been discovered to boost ROS and ER stress inside cancer cells,[127] as well as ICD induction.[47] The fluorescence imaging and flow cytometry data indicated that **Au-8**-treated HCT116 cells conferred a strong calreticulin (CRT) surface exposure, which is known to deliver robust pro-

https://doi.org/10.1021/jacs.5c19777
J. Am. Chem. Soc. XXXX, XXX, XXX−XXX

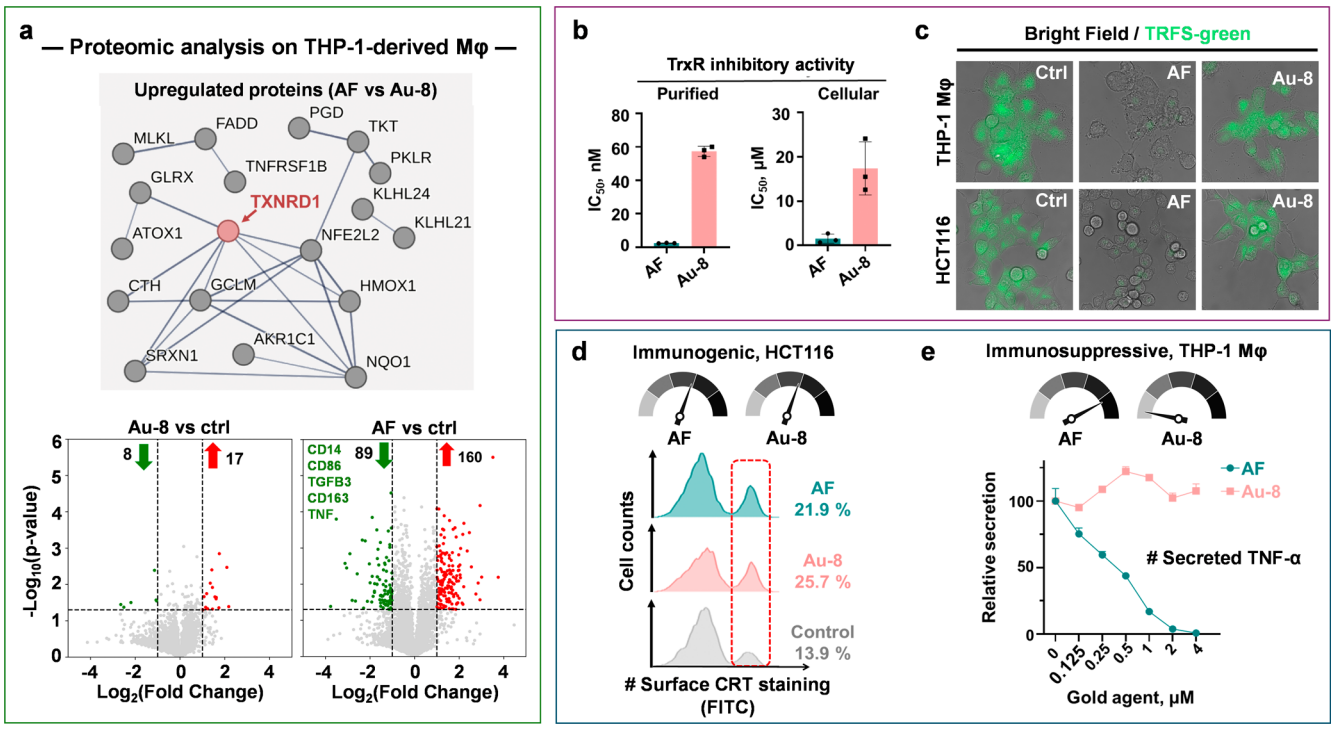

Figure 5. Au-8 reprogrammed immunomodulatory function. (a) Proteomic profiling of THP-1-derived Mφ treated with 1 μM auranofin or **Au-8** for 24 h. Three biological replicates were applied. The protein−protein interaction network was generated by STRING.[123] Proteins are represented as dots with gene names, and the lines represent the experimentally verified interactions. The thickness of each line reflects the strength of the data support. The most connected protein, *TRXNRD1* (TrxR1), was highlighted. The volcano plots in the lower part show the relative changes of each gold treatment relative to the untreated control (Ctrl). Monocytic or macrophage markers only reduced by auranofin have been listed in the plot. (b) The TrxR inhibitory IC_{50} based on purified human TrxR1 or cell lysates were measured after a 0.5-h incubation of the gold compounds with the enzyme or with HCT116 cells. (c) Microscopy imaging of cellular TrxR activity using TRFS-green probe in the living HCT116 cells or THP-1-derived Mφ under indicated treatments. One × IC_{50} of each gold compound for the indicated cell types was used for a 0.5-h incubation followed staining by TRFS-green at 10 μM. Images were shown as the merged picture of a bright field and a green fluorescence channel. (d) Flow cytometry experiments quantifying the HCT116 cell surface CRT under indicated conditions. Gold compounds were used at a 1 × IC_{50}. (e) TNF-α secretion by THP-1-derived Mφ was measured using ELISA under the treatment of each gold compound. The dashboards in d and e were created with Biorender.com.

phagocytic signals to myeloid cells, including the engulfment by dendritic cells to initiate ICD and direct activation of natural killer (NK) cells.[128,129] The proportion of CRT-positive cells in the **Au-8** group is 25.7% and that in auranofin group is 21.9% (Figure 5d and S15), compared to 13.9% of the control group, suggesting similarly high immunogenic potency of the two gold compounds.[129,130] In contrast, we discovered a huge difference between the two gold compounds toward THP-1-derived macrophage in the TNF-α secretion at their sublethal concentrations. As shown in Figure 5e, consistent with the previous reports, auranofin inhibited TNF-α secretion beginning at a low concentration of 0.125 μM, exhibiting an inhibitory IC_{50} of 0.39 μM, which is approximately one-fiftieth (1/50) of its cytotoxicity against THP-1 macrophage (IC_{50} = 18.9 μM) and one-seventh that against HCT116 cell (IC_{50} = 2.90 μM). This aligns with the truth that auranofin can interfere with macrophage function even at nontoxic doses. In contrast, **Au-8** not only failed to inhibit TNF-α secretion but appeared to increase its levels at concentrations below 1 μM; it showed negligible inhibitory activity up to 4 μM, a concentration approaching its cytotoxic half-maximal inhibitory concentration for cancer cells such as HCT116. This indicates a potential therapeutic window enabling selective antitumor efficacy without compromising the immune cell function.

Au-8, but Not Auranofin, Boosts Immunogenic Phagocytosis and Cytotoxicity in Human Primary Immune Cells

We further evaluated the two compounds on peripheral blood mononuclear cells (PBMCs) isolated from the whole blood of healthy human donors (Figure 6a). Cytotoxicity assay revealed that **Au-8** displayed an average of 2.5-fold lower cytotoxicity than auranofin across five batches of PBMCs (Figure 6b, left). Additionally, CD14+ monocytes, which are the largest type of white blood cells in humans and can differentiate into macrophages and dendritic cells, playing a crucial role in both innate and adaptive immune responses, were further isolated for analysis. Cytotoxicity studies again demonstrated that **Au-8** showed 2.5-fold less cytotoxicity compared to auranofin in these monocytes (Figure 6b, right). Therefore, while the two compounds show similar cytotoxicity to cancer cells, their distinct mechanisms of inducing ROS result in a lower toxicity of **Au-8** to immune cells compared to auranofin.

Subsequently, we assessed the immunological phagocytic capability of isolated human PBMCs. Phagocytosis is a key mechanism of the innate immune defense and serves as one of the initial responses to infection as well as a critical initiator of the adaptive immune response. This experiment utilized pHrodo particles, which are nonemissive in the medium but become highly fluorescent in the acidic environment of late

https://doi.org/10.1021/jacs.5c19777
J. Am. Chem. Soc. XXXX, XXX, XXX−XXX

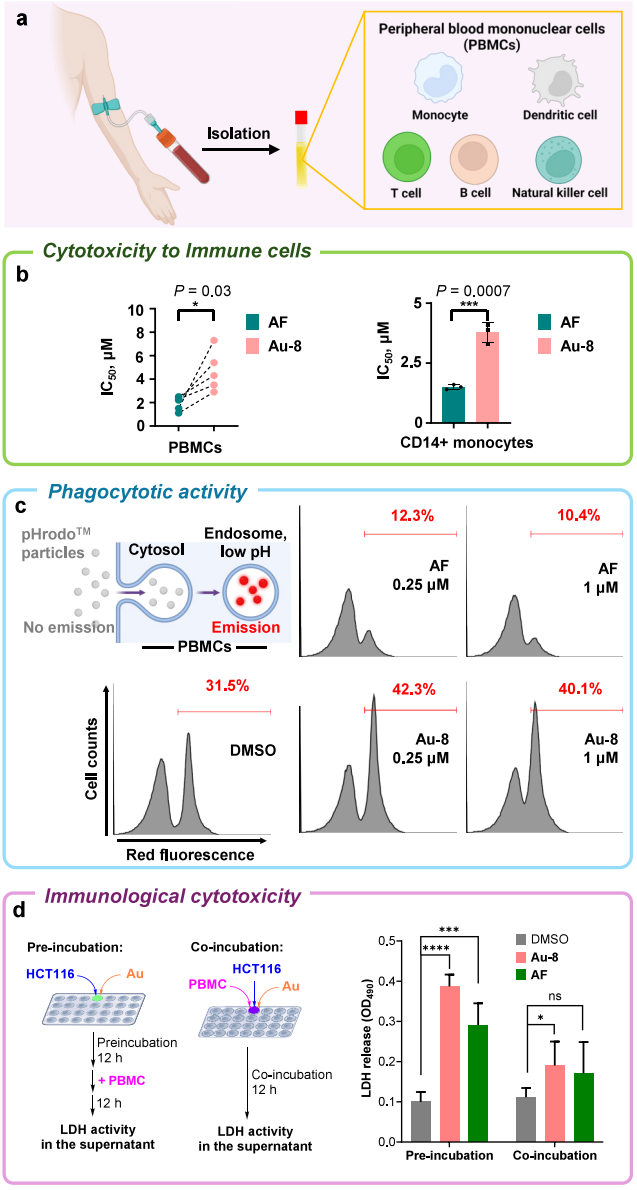

Figure 6. Effects of Au Compounds on PBMCs. (a) Description for isolation of PBMCs (created with Biorender.com). (b) Cytotoxicity of gold compounds toward human PBMCs and CD14+ monocytes isolated from the blood of healthy donors. For the PBMC, cells isolated from the blood of five healthy donors were tested. For CD14+ monocytes, triplicates were tested using cells from a single donor. (c) Phagocytosis assays using pHrodo particles and PBMCs. The percentage of positive-stained cells were shown. (d) The immunogenic cytotoxicity (as revealed from the activity of released LDH from dead cells) after preincubation of HCT116 cells and **Au-8** or **AF** at their 1 × IC_{50} concentration for 12 h, followed by adding PBMC for another 12 h incubation, or direct coincubation of HCT116 cells, PBMCs, and **Au-8** or **AF** for a total 12 h incubation.

endosomes once they are internalized by immune cells (Figure 6c). After human PBMCs were treated by different concentrations of gold compounds for 12 h, followed by additional incubation with pHrodo particle for 30 min, the cells were analyzed by flow cytometry. Data in Figure 6c showed that the control group exhibited 31.5% of the phagocytosis-positive cells, which decreased to 12.3% and 10.4% under 0.25 μM and 1 μM of auranofin treatment (Figure 6c), correlating with its potent inhibitory effects toward cytokine release under similar concentrations (Figure 5e). By contrast, **Au-8** further boosted phagocytosis to over 40% under the same treatment conditions, possibly due to its non-TrxR-associated prooxidant activity, which boosted phagocytes in PBMCs.[131]

To further investigate whether **Au-8** can activate immune cells to target and eliminate cancer cells, the following experiments were performed. At first, HCT116 cells were pretreated with **Au-8** or auranofin for 12 h to allow exposure of immunogenic signals, followed by adding PBMCs (ratio of 20:1 to HCT116 cells) for another 12 h incubation. Then cell killing effects were examined by measuring the activity of lactate dehydrogenase (LDH) released from dead or damaged cells. As the results show in Figure 6d and S16, while **Au-8** and auranofin did not show direct cytotoxicity to cancer cells or PBMCs, the pretreatment significantly boosted the cytotoxicity of PBMCs to cancer cells, with a slightly higher activity of **Au-8** than auranofin.

However, when HCT116 cells, PBMCs, and gold compounds were directly combined in a single mixture and incubated for 12 h, the two gold complexes exhibited different effects. As shown in Figure 6d, auranofin resulted in slightly higher LDH activity in the combination group. However, this increase was not statistically significant and was due to its direct cytotoxicity toward PBMCs (Figure S16) rather than any immunogenic properties, suggesting that auranofin might damage immune cells before exerting any potential immunogenic activity. In contrast, **Au-8** led to a significantly higher LDH content in the combination group. In the absence of either HCT116 cells or PBMCs, no significant increase in the LDH content was observed following **Au-8** treatment (Figure S16). This suggests that the observed cytotoxicity in the combination is due to **Au-8**'s ability to activate immune responses, which target and eliminate cancer cells.

Au-8 Reprograms the Immunomodulatory Function in Vivo

To examine the possible immunological activity in vivo, immunocompetent mouse models were employed. In brief, the mice bearing MC38 colorectal tumor xenografts were treated with solvent, auranofin, or **Au-8** (both gold compounds at 10 mg/kg) once per 2 days. Results showed that both compounds can inhibit tumor growth with an inhibition rate of 82% for auranofin and 90% for **Au-8** after 14 days of treatment without mouse death or body weight loss (Figures 7a, b and S17). It appears that the inhibition pattens of the two compounds are different. Auranofin started to inhibit tumor growth since the first injection (measured on day 2) but it only slows down the tumor growth. However, In the **Au-8** treatment group, there was no inhibition after the first 3 times treatment, but after 6 days, the tumor volume started to decline until day 14 of sacrifice. This prompts us to examine whether the tumor immunity plays a role for the observed tumor inhibition.

To achieve this, we stained the cells from isolated tumors with immune cell markers. The results (Figure 7c–e) indicated that tumors treated with **Au-8** exhibited significant immune activation, evidenced by more than a 3-fold increase in the expression of inflammatory INF-γ and significant increase of CD11b+. In contrast, auranofin treatment did not result in changes in INF-γ, although it appeared that there was an increase in the number of CD4+ T cells. However, further analysis incorporating Foxp3 revealed that the increase in CD4+ T cells was primarily due to a significant upregulation of

https://doi.org/10.1021/jacs.5c19777
J. Am. Chem. Soc. XXXX, XXX, XXX−XXX

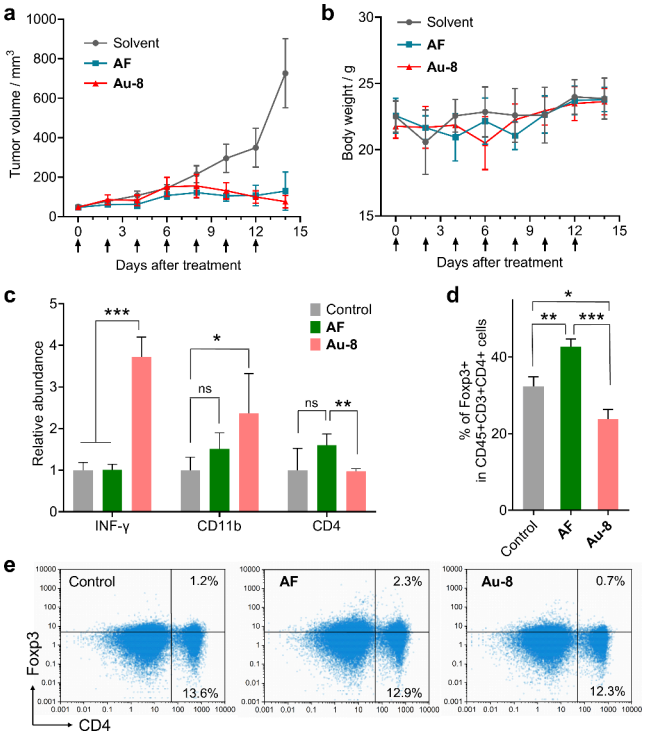

Figure 7. Antitumor activities in immunocompetent mouse models. (a, b) The tumor volume (a) and body weight (b) after treating mice bearing MC38 cells by **Au-8** or auranofin at 10 mg/kg once per 2 days for a successive 14 days. Each group contains 7 mice. The arrows indicate drug treatment. (c–e) Detection of immune cell markers within the tumors, showing altered expression of INF-γ, CD4, CD11b after treatment (c), the varied expression of immune suppressive CD4+Foxp3+ T_{reg} cells (d, e).

CD4+Foxp3+ regulatory T cells (T_{reg}), which contribute to an immune-suppressive environment.[132] In contrast, T_{reg} cells in the **Au-8** group is downregulated. Therefore, catalytically active **Au-8** can indeed effectively reprogram the immunomodulatory function of auranofin and suppress tumor growth under in vivo conditions.

CONCLUSION

For thiol-reactive gold complexes, intracellular ligand exchange often leads to the primary targeting of TrxR, as this type of protein carries Cys/Sec residues with a high gold-binding affinity. Gold complexes may strongly inhibit TrxR1 even at nontoxic concentrations. Since many immune cells heavily rely on the proper function of TrxR1, especially during their activated states, using gold drugs such as auranofin in cancer therapy may suppress the immune system before exerting cytotoxic/immunogenic effects on cancer cells. As our data showed above, auranofin at merely one-seventh of the cytotoxic IC_{50} concentration suppressed cytokine release from human macrophages. This raises a significant concern that repurposing auranofin for cancer therapy may strongly dampen the patients' anticancer immunity without exerting its potential immunogenic activity on tumor cells.

In this study, we discovered that NHC-Au-Cl complexes with bulky substituents, such as **Au-3** and **Au-8**, can display catalytic activities even in the presence of millimolar amounts of GSH and effectively facilitate the oxidation of NADH to NAD^+. Remarkably, although **Au-8** exhibits a much lower cellular uptake compared to auranofin, it demonstrates comparable cytotoxicity against cancer cells by acting as an ROS-promoting agent without inhibiting TrxR1. This mechanism substantially reduces its toxicity toward immune cells and redirects the immune response from immunosuppression toward activation. Such properties could potentially enhance therapeutic applications of gold compounds in immunotherapy combinations. We anticipate these findings will inspire further exploration into ligands that impart novel catalytic functions and associated bioactivities to gold complexes for drug development.

ASSOCIATED CONTENT

Supporting Information

The Supporting Information is available free of charge at https://pubs.acs.org/doi/10.1021/jacs.5c19777.

All the experimental procedures, the synthesis steps, list of the analysis data of the new compounds, supplementary references, schemes, tables, and figures (PDF)

Accession Codes

Deposition Number 2421111 contains the supplementary crystallographic data for this paper. These data can be obtained free of charge via the joint Cambridge Crystallographic Data Centre (CCDC) and Fachinformationszentrum Karlsruhe Access Structures service.

AUTHOR INFORMATION

Corresponding Authors

Taotao Zou − *State Key Laboratory of Anti-Infective Drug Discovery and Development, Guangdong Key Laboratory of Chiral Molecule and Drug Discovery, and School of Pharmaceutical Sciences, Sun Yat-Sen University, Guangzhou 510006, China; Senior Department of Nephrology, Chinese PLA General Hospital, State Key Laboratory of Kidney Diseases, Beijing 100853, China;* orcid.org/0000-0001-9129-4398; Email: zoutt3@mail.sysu.edu.cn

Jinsai Shang − *School of Basic Medical Sciences, State Key Laboratory of Respiratory Disease, Guangzhou National Laboratory, Guangzhou Medical University, Guangzhou 511436, China;* orcid.org/0009-0004-4557-2974; Email: shang_jinsai@gzlab.ac.cn

Xiaolin Xiong − *State Key Laboratory of Anti-Infective Drug Discovery and Development, Guangdong Key Laboratory of Chiral Molecule and Drug Discovery, and School of Pharmaceutical Sciences, Sun Yat-Sen University, Guangzhou 510006, China*; Email: xiongxlin@mail.sysu.edu.cn

Ke-Bin Huang − *Key Laboratory for Chemistry and Molecular Engineering of Medicinal Resources (Ministry of Education of China), School of Chemistry and Pharmaceutical Sciences, Guangxi Normal University, Guilin 541004, China;* orcid.org/0000-0003-4773-4442; Email: kbhuang@mailbox.gxnu.edu.cn

Authors

Zhi Zhong − *State Key Laboratory of Anti-Infective Drug Discovery and Development, Guangdong Key Laboratory of Chiral Molecule and Drug Discovery, and School of Pharmaceutical Sciences, Sun Yat-Sen University, Guangzhou 510006, China*

Haitao Liu − *State Key Laboratory of Anti-Infective Drug Discovery and Development, Guangdong Key Laboratory of Chiral Molecule and Drug Discovery, and School of*

Pharmaceutical Sciences, Sun Yat-Sen University, Guangzhou 510006, China

Qiong Wu − *School of Basic Medical Sciences, State Key Laboratory of Respiratory Disease, Guangzhou National Laboratory, Guangzhou Medical University, Guangzhou 511436, China*

Bei Cao − *College of Education Sciences, The Hong Kong University of Science and Technology (Guangzhou), Guangzhou 511453, China*

Yujiao Peng − *State Key Laboratory of Anti-Infective Drug Discovery and Development, Guangdong Key Laboratory of Chiral Molecule and Drug Discovery, and School of Pharmaceutical Sciences, Sun Yat-Sen University, Guangzhou 510006, China*

Moyi Liu − *State Key Laboratory of Anti-Infective Drug Discovery and Development, Guangdong Key Laboratory of Chiral Molecule and Drug Discovery, and School of Pharmaceutical Sciences, Sun Yat-Sen University, Guangzhou 510006, China*

Liang-Mei Yang − *Key Laboratory for Chemistry and Molecular Engineering of Medicinal Resources (Ministry of Education of China), School of Chemistry and Pharmaceutical Sciences, Guangxi Normal University, Guilin 541004, China*

Yue Lin − *School of Basic Medical Sciences, State Key Laboratory of Respiratory Disease, Guangzhou National Laboratory, Guangzhou Medical University, Guangzhou 511436, China*

Complete contact information is available at: https://pubs.acs.org/10.1021/jacs.5c19777

Author Contributions

‡Z.Z., H.L., Q.W., and B.C. contributed equally.

Notes

The authors declare no competing financial interest.

■ ACKNOWLEDGMENTS

This work was financially supported by the National Natural Science Foundation of China (No. 22377154, 22122706, 32100058, 82170473), Major Program of Guangzhou National Laboratory (GZNL2023A02012, GZNL2025C02004), Guangdong Science and Technology Department (No. 2019QN01C125, 2021QN020451), Guangdong Basic and Applied Basic Research Foundation (No. 2024A1515010721, 2024B1515040028), Guangzhou Science and Technology Projects (2024A04J6478, 2024A04J3287), and Guangdong Provincial Key Lab of Chiral Molecule and Drug Discovery (No. 2023B1212060022).

■ REFERENCES

(1) Sies, H.; Belousov, V. V.; Chandel, N. S.; Davies, M. J.; Jones, D. P.; Mann, G. E.; Murphy, M. P.; Yamamoto, M.; Winterbourn, C. Defining roles of specific reactive oxygen species (ROS) in cell biology and physiology. *Nat. Rev. Mol. Cell Biol.* **2022**, *23*, 499−515.

(2) Sabharwal, S. S.; Schumacker, P. T. Mitochondrial ROS in cancer: initiators, amplifiers or an Achilles' heel? *Nat. Rev. Cancer* **2014**, *14*, 709−721.

(3) Ralph, S. J.; Nozuhur, S.; Alhulais, R. A.; Rodríguez-Enríquez, S.; Moreno-Sánchez, R. Repurposing drugs as pro-oxidant redox modifiers to eliminate cancer stem cells and improve the treatment of advanced stage cancers. *Med. Res. Rev.* **2019**, *39*, 2397−2426.

(4) Hayes, J. D.; Dinkova-Kostova, A. T.; Tew, K. D. Oxidative Stress in Cancer. *Cancer Cell* **2020**, *38*, 167−197.

(5) Bindoli, A.; Rigobello, M. P.; Scutari, G.; Gabbiani, C.; Casini, A.; Messori, L. Thioredoxin Reductase: A Target for Gold Compounds Acting as Potential Anticancer Drugs. *Coord. Chem. Rev.* **2009**, *253*, 1692−1707.

(6) Tang, Z.; Kang, B.; Li, C.; Chen, T.; Zhang, Z. GEPIA2: an enhanced web server for large-scale expression profiling and interactive analysis. *Nucleic Acids Res.* **2019**, *47*, W556−W560.

(7) Berglund, L.; Björling, E.; Oksvold, P.; Fagerberg, L.; Asplund, A.; Al-Khalili Szigyarto, C.; Persson, A.; Ottosson, J.; Wernérus, H.; Nilsson, P.; Lundberg, E.; Sivertsson, Å.; Navani, S.; Wester, K.; Kampf, C.; Hober, S.; Pontén, F.; Uhlén, M. A Genecentric Human Protein Atlas for Expression Profiles Based on Antibodies. *Mol. Cell. Proteomics* **2008**, *7*, 2019−2027.

(8) Uhlen, M.; Zhang, C.; Lee, S.; Sjöstedt, E.; Fagerberg, L.; Bidkhori, G.; Benfeitas, R.; Arif, M.; Liu, Z.; Edfors, F.; Sanli, K.; von Feilitzen, K.; Oksvold, P.; Lundberg, E.; Hober, S.; Nilsson, P.; Mattsson, J.; Schwenk, J. M.; Brunnström, H.; Glimelius, B.; Sjöblom, T.; Edqvist, P.-H.; Djureinovic, D.; Micke, P.; Lindskog, C.; Mardinoglu, A.; Ponten, F. A pathology atlas of the human cancer transcriptome. *Science* **2017**, *357*, No. eaan2507.

(9) Liu, M.; Liu, H.; Yang, Y.; Xiong, X.; Zou, T. Subcellular Photocatalysis Enables Tumor-Targeted Inhibition of Thioredoxin Reductase I by Organogold(I) Complexes. *J. Am. Chem. Soc.* **2025**, *147*, 15719−15731.

(10) Sadler, P. J.; Sue, R. E. The Chemistry of Gold Drugs. *Met.-Based Drugs* **1994**, *1*, 107−144.

(11) Ott, I. On the Medicinal Chemistry of Gold Complexes as Anticancer Drugs. *Coord. Chem. Rev.* **2009**, *253*, 1670−1681.

(12) Nobili, S.; Mini, E.; Landini, I.; Gabbiani, C.; Casini, A.; Messori, L. Gold Compounds as Anticancer Agents: Chemistry, Cellular Pharmacology, and Preclinical Studies. *Med. Res. Rev.* **2010**, *30*, 550−580.

(13) Gasser, G.; Ott, I.; Metzler-Nolte, N. Organometallic Anticancer Compounds. *J. Med. Chem.* **2011**, *54*, 3−25.

(14) Meyer, A.; Bagowski, C. P.; Kokoschka, M.; Stefanopoulou, M.; Alborzinia, H.; Can, S.; Vlecken, D. H.; Sheldrick, W. S.; Wölfl, S.; Ott, I. On the Biological Properties of Alkynyl Phosphine Gold(I) Complexes. *Angew. Chem., Int. Ed.* **2012**, *51*, 8895−8899.

(15) Berners-Price, S. J.; Barnard, P. J. Therapeutic Gold Compounds. In *Ligand Design in Medicinal Inorganic Chemistry*; John Wiley & Sons, Ltd., 2014; pp 227−256.

(16) Casini, A.; Wai-Yin Sun, R.; Ott, I. Medicinal Chemistry of Gold Anticancer Metallodrugs. *Metallo-Drugs: Development and Action of Anticancer Agents*; Sigel, A., Sigel, H., Freisinger, E., Sigel, R. K. O., Eds.; De Gruyter, 2018; Chapter 7, pp 199−218.

(17) Zhou, X.-Q.; Carbo-Bague, I.; Siegler, M. A.; Hilgendorf, J.; Basu, U.; Ott, I.; Liu, R.; Zhang, L.; Ramu, V.; Ijzerman, A. P.; Bonnet, S. Rollover Cyclometalation vs Nitrogen Coordination in Tetrapyridyl Anticancer Gold(III) Complexes: Effect on Protein Interaction and Toxicity. *JACS Au* **2021**, *1*, 380−395.

(18) Gamberi, T.; Pratesi, A.; Messori, L.; Massai, L. Proteomics as a tool to disclose the cellular and molecular mechanisms of selected anticancer gold compounds. *Coord. Chem. Rev.* **2021**, *438*, 213905.

(19) Marciano, Y.; del Solar, V.; Nayeem, N.; Dave, D.; Son, J.; Contel, M.; Ulijn, R. V. Encapsulation of Gold-Based Anticancer Agents in Protease-Degradable Peptide Nanofilaments Enhances Their Potency. *J. Am. Chem. Soc.* **2023**, *145*, 234−246.

(20) Cosottini, L.; Geri, A.; Ghini, V.; Mannelli, M.; Zineddu, S.; Di Paco, G.; Giachetti, A.; Massai, L.; Severi, M.; Gamberi, T.; Rosato, A.; Turano, P.; Messori, L. Unlocking the Power of Human Ferritin: Enhanced Drug Delivery of Aurothiomalate in A2780 Ovarian Cancer Cells. *Angew. Chem., Int. Ed.* **2024**, *63*, No. e202410791.

(21) Casini, A.; Pöthig, A. Metals in Cancer Research: Beyond Platinum Metallodrugs. *ACS Cent. Sci.* **2024**, *10*, 242−250.

(22) Jiang, J.; Xiong, X.; Zou, T. Modulating the Chemical Reactivity of Gold Complexes in Living Systems: From Concept to Biomedical Applications. *Acc. Chem. Res.* **2023**, *56*, 1043−1056.

(23) Babu, T.; Levine, M. S.; Acharya, S.; Maier, E. Y.; Sessler, J. L. Three Is Better than One: A Multimetal Complex that Triggers

Immunogenic Cell Death. *Angew. Chem., Int. Ed.* **2025**, *64*, No. e202514351.
(24) Lim, J. Y.; Yeo, C. I.; Yow, Y.-Y. Golden keys to inflammation: decoding the anti-inflammatory mechanisms of gold(I) and gold(III) complexes (2010-present). *Coord. Chem. Rev.* **2026**, *549*, 217354.
(25) Lu, Y.; Ma, X.; Chang, X.; Liang, Z.; Lv, L.; Shan, M.; Lu, Q.; Wen, Z.; Gust, R.; Liu, W. Recent development of gold(I) and gold(III) complexes as therapeutic agents for cancer diseases. *Chem. Soc. Rev.* **2022**, *51*, 5518−5556.
(26) Mertens, R. T.; Gukathasan, S.; Arojojoye, A. S.; Olelewe, C.; Awuah, S. G. Next Generation Gold Drugs and Probes: Chemistry and Biomedical Applications. *Chem. Rev.* **2023**, *123*, 6612−6667.
(27) Wang, Y.; Cao, B.; Wang, Q.; Zhong, S.; Fang, X.; Wang, J.; Chan, A. S. C.; Xiong, X.; Zou, T. Ligand supplementation restores the cancer therapy efficacy of the antirheumatic drug auranofin from serum inactivation. *Nat. Commun.* **2025**, *16*, 7347.
(28) Berners-Price, S. J.; Mirabelli, C. K.; Johnson, R. K.; Mattern, M. R.; McCabe, F. L.; Faucette, L. F.; Sung, C.-M.; Mong, S.-M.; Sadler, P. J.; Crooke, S. T. In Vivo Antitumor Activity and in Vitro Cytotoxic Properties of Bis[1,2-bis(diphenylphosphino)ethane]gold-(I) Chloride. *Cancer Res.* **1986**, *46*, 5486−5493.
(29) Messori, L.; Abbate, F.; Marcon, G.; Orioli, P.; Fontani, M.; Mini, E.; Mazzei, T.; Carotti, S.; O'Connell, T.; Zanello, P. Gold(III) Complexes as Potential Antitumor Agents: Solution Chemistry and Cytotoxic Properties of Some Selected Gold(III) Compounds. *J. Med. Chem.* **2000**, *43*, 3541−3548.
(30) Fernández-Gallardo, J.; Elie, B. T.; Sadhukha, T.; Prabha, S.; Sanaú, M.; Rotenberg, S. A.; Ramos, J. W.; Contel, M. Heterometallic titanium-gold complexes inhibit renal cancer cells in vitro and in vivo. *Chem. Sci.* **2015**, *6*, 5269−5283.
(31) McCall, R.; Miles, M.; Lascuna, P.; Burney, B.; Patel, Z.; Sidoran, K. J.; Sittaramane, V.; Kocerha, J.; Grossie, D. A.; Sessler, J. L.; Arumugam, K.; Arambula, J. F. Dual targeting of the cancer antioxidant network with 1,4-naphthoquinone fused Gold(i) N-heterocyclic carbene complexes. *Chem. Sci.* **2017**, *8*, 5918−5929.
(32) Wirmer-Bartoschek, J.; Bendel, L. E.; Jonker, H. R. A.; Grün, J. T.; Papi, F.; Bazzicalupi, C.; Messori, L.; Gratteri, P.; Schwalbe, H. Solution NMR Structure of a Ligand/Hybrid-2-G-Quadruplex Complex Reveals Rearrangements that Affect Ligand Binding. *Angew. Chem., Int. Ed.* **2017**, *56*, 7102−7106.
(33) Bertrand, B.; Fernandez-Cestau, J.; Angulo, J.; Cominetti, M. M. D.; Waller, Z. A. E.; Searcey, M.; O'Connell, M. A.; Bochmann, M. Cytotoxicity of Pyrazine-Based Cyclometalated (ĈNpẑC)Au(III) Carbene Complexes: Impact of the Nature of the Ancillary Ligand on the Biological Properties. *Inorg. Chem.* **2017**, *56*, 5728−5740.
(34) Wragg, D.; de Almeida, A.; Bonsignore, R.; Kühn, F. E.; Leoni, S.; Casini, A. On the Mechanism of Gold/NHC Compounds Binding to DNA G-Quadruplexes: Combined Metadynamics and Biophysical Methods. *Angew. Chem., Int. Ed.* **2018**, *57*, 14524−14528.
(35) Sze, J. H.; Raninga, P. V.; Nakamura, K.; Casey, M.; Khanna, K. K.; Berners-Price, S. J.; Di Trapani, G.; Tonissen, K. F. Anticancer activity of a Gold(I) phosphine thioredoxin reductase inhibitor in multiple myeloma. *Redox Biol.* **2020**, *28*, 101310.
(36) Guarra, F.; Terenzi, A.; Pirker, C.; Passannante, R.; Baier, D.; Zangrando, E.; Gómez-Vallejo, V.; Biver, T.; Gabbiani, C.; Berger, W.; Llop, J.; Salassa, L. ^{124}I Radiolabeling of a Au^{III}-NHC Complex for In Vivo Biodistribution Studies. *Angew. Chem., Int. Ed.* **2020**, *59*, 17130−17136.
(37) Zhang, J.-J.; Abu el Maaty, M. A.; Hoffmeister, H.; Schmidt, C.; Muenzner, J. K.; Schobert, R.; Wölfl, S.; Ott, I. A Multitarget Gold(I) Complex Induces Cytotoxicity Related to Aneuploidy in HCT-116 Colorectal Carcinoma Cells. *Angew. Chem., Int. Ed.* **2020**, *59*, 16795−16800.
(38) Xu, Z.; Lu, Q.; Shan, M.; Jiang, G.; Liu, Y.; Yang, Z.; Lu, Y.; Liu, W. NSAID-Au(I) Complexes Induce ROS-Driven DAMPs and Interpose Inflammation to Stimulate the Immune Response against Ovarian Cancer. *J. Med. Chem.* **2023**, *66*, 7813−7833.
(39) Moreno-Alcántar, G.; Picchetti, P.; Casini, A. Gold Complexes in Anticancer Therapy: From New Design Principles to Particle-Based Delivery Systems. *Angew. Chem., Int. Ed.* **2023**, *62*, No. e202218000.
(40) Babu, T.; Ghareeb, H.; Basu, U.; Schueffl, H.; Theiner, S.; Heffeter, P.; Koellensperger, G.; Metanis, N.; Gandin, V.; Ott, I.; Schmidt, C.; Gibson, D. Oral Anticancer Heterobimetallic Pt^{IV}-Au^{I} Complexes Show High In Vivo Activity and Low Toxicity. *Angew. Chem., Int. Ed.* **2023**, *62*, No. e202217233.
(41) Zhou, X.-Q.; Abyar, S.; Carbo-Bague, I.; Wang, L.; Turck, S.; Siegler, M. A.; Basu, U.; Ott, I.; Liu, R.; IJzerman, A. P.; Bonnet, S. Multitarget Thiol-Activated Tetrapyridyl Gold(III) Complexes for Hypoxic Cancer Therapy. *CCS Chem.* **2024**, *6*, 783−797.
(42) Kapitza, P.; Scherfler, A.; Salcher, S.; Sopper, S.; Cziferszky, M.; Wurst, K.; Gust, R. Reaction Behavior of [1,3-Diethyl-4,5-diphenyl-1H-imidazol-2-ylidene] Containing Gold(I/III) Complexes against Ingredients of the Cell Culture Medium and the Meaning on the Potential Use for Cancer Eradication Therapy. *J. Med. Chem.* **2023**, *66*, 8238−8250.
(43) Ahad, A.; Aftab, F.; Michel, A.; Lewis, J. S.; Contel, M. Development of immunoliposomes containing cytotoxic gold payloads against HER2-positive breast cancers. *RSC Med. Chem.* **2024**, *15*, 139−150.
(44) Gukathasan, S.; Olelewe, C.; Ratliff, L.; Kim, J. H.; Ackerman, A. M.; McCorkle, J. R.; Parkin, S.; Kwakye, G. F.; Kolesar, J. M.; Awuah, S. G. Chemoproteomic Profiling of a Carbon-Stabilized Gold(III) Macrocycle Reveals Cellular Engagement with HMOX2. *J. Med. Chem.* **2025**, *68*, 5687−5698.
(45) Babak, M. V.; Chong, K. R.; Rapta, P.; Zannikou, M.; Tang, H. M.; Reichert, L.; Chang, M. R.; Kushnarev, V.; Heffeter, P.; Meier-Menches, S. M.; Lim, Z. C.; Yap, J. Y.; Casini, A.; Balyasnikova, I. V.; Ang, W. H. Interfering with Metabolic Profile of Triple-Negative Breast Cancers Using Rationally Designed Metformin Prodrugs. *Angew. Chem., Int. Ed.* **2021**, *60*, 13405−13413.
(46) Sen, S.; Hufnagel, S.; Maier, E. Y.; Aguilar, I.; Selvakumar, J.; DeVore, J. E.; Lynch, V. M.; Arumugam, K.; Cui, Z.; Sessler, J. L.; Arambula, J. F. Rationally Designed Redox-Active Au(I) N-Heterocyclic Carbene: An Immunogenic Cell Death Inducer. *J. Am. Chem. Soc.* **2020**, *142*, 20536−20541.
(47) Freire Boullosa, L.; Van Loenhout, J.; Flieswasser, T.; De Waele, J.; Hermans, C.; Lambrechts, H.; Cuypers, B.; Laukens, K.; Bartholomeus, E.; Siozopoulou, V.; De Vos, W. H.; Peeters, M.; Smits, E. L. J.; Deben, C. Auranofin reveals therapeutic anticancer potential by triggering distinct molecular cell death mechanisms and innate immunity in mutant p53 non-small cell lung cancer. *Redox Biol.* **2021**, *42*, 101949.
(48) Levine, M. S.; Sen, S.; Maier, E. Y.; Mota, M.; Won, M.; Li, J.; Arambula, J. F.; Lynch, V. M.; Kim, J. S.; DePinho, R. A.; Iverson, B.; Sessler, J. L. Long-Lived Immunogenic Cell Death Induced by a Water-Soluble Redox Active Au(I) Bis-N-Heterocyclic Carbene. *J. Am. Chem. Soc.* **2025**, *147*, 23574−23582.
(49) Chang, M. R.; Matnurov, E. M.; Wu, C.; Arakelyan, J.; Choe, H.-J.; Kushnarev, V.; Yap, J. Y.; Soo, X. X.; Chow, M. J.; Berger, W.; Ang, W. H.; Babak, M. V. Leveraging Immunogenic Cell Death to Enhance the Immune Response against Malignant Pleural Mesothelioma Tumors. *J. Am. Chem. Soc.* **2025**, *147*, 7908−7920.
(50) Schütze, N.; Fritsche, J.; Ebert-Dümig, R.; Schneider, D.; Köhrle, J.; Andreesen, R.; Kreutz, M.; Jakob, F. The selenoprotein thioredoxin reductase is expressed in peripheral blood monocytes and THP1 human myeloid leukemia cells - regulation by 1,25-dihydroxyvitamin D3 and selenite. *BioFactors* **1999**, *10*, 329−338.
(51) Trávníček, Z.; Štarha, P.; Vančo, J.; Šilha, T.; Hošek, J.; Suchý, P., Jr; Pražanová, G. Anti-inflammatory Active Gold(I) Complexes Involving 6-Substituted-Purine Derivatives. *J. Med. Chem.* **2012**, *55*, 4568−4579.
(52) Abu Hariri, H.; Braunstein, I.; Salti, T.; Glaser, F.; Gefen, T.; Geva-Zatorsky, N.; Ziv, T.; Benhar, M. Global Thiol Proteome Analysis Provides Novel Insights into the Macrophage Inflammatory Response and Its Regulation by the Thioredoxin System. *Antioxid. Redox Signaling* **2022**, *38*, 388−402.

https://doi.org/10.1021/jacs.5c19777
J. Am. Chem. Soc. XXXX, XXX, XXX−XXX

(53) Blanco, A.; Coronado, R. A.; Arun, N.; Ma, K.; Dar, R. D.; Kieffer, C. Monocyte to macrophage differentiation and changes in cellular redox homeostasis promote cell type-specific HIV latency reactivation. *Proc. Natl. Acad. Sci. U. S. A.* **2024**, *121*, No. e2313823121.
(54) Muri, J.; Heer, S.; Matsushita, M.; Pohlmeier, L.; Tortola, L.; Fuhrer, T.; Conrad, M.; Zamboni, N.; Kisielow, J.; Kopf, M. The thioredoxin-1 system is essential for fueling DNA synthesis during T-cell metabolic reprogramming and proliferation. *Nat. Commun.* **2018**, *9*, 1851.
(55) Sen, S.; Won, M.; Levine, M. S.; Noh, Y.; Sedgwick, A. C.; Kim, J. S.; Sessler, J. L.; Arambula, J. F. Metal-based anticancer agents as immunogenic cell death inducers: the past, present, and future. *Chem. Soc. Rev.* **2022**, *51*, 1212−1233.
(56) Zhao, Z.; Zhang, S.; Jiang, N.; Zhu, W.; Song, D.; Liu, S.; Yu, W.; Bai, Y.; Zhang, Y.; Wang, X.; Zhong, X.; Guo, H.; Guo, Z.; Yang, R.; Li, J. P. Patient-derived Immunocompetent Tumor Organoids: A Platform for Chemotherapy Evaluation in the Context of T-cell Recognition. *Angew. Chem., Int. Ed.* **2024**, *63*, No. e202317613.
(57) Xue, Q.; Yu, W.; Li, J. P.; He, C.; Guo, Z. Revealing the nature of Pt-based immunotherapy through the lens of neoantigens in cancer. *Sci. Bull.* **2024**, *69*, 2314−2318.
(58) Peng, K.; Zheng, Y.; Xia, W.; Mao, Z.-W. Organometallic anti-tumor agents: targeting from biomolecules to dynamic bioprocesses. *Chem. Soc. Rev.* **2023**, *52*, 2790−2832.
(59) Zou, J. X.; Chang, M. R.; Kuznetsov, N. A.; Kee, J. X.; Babak, M. V.; Ang, W. H. Metal-based immunogenic cell death inducers for cancer immunotherapy. *Chem. Sci.* **2025**, *16*, 6160−6187.
(60) Huang, K.-B.; Wang, F.-Y.; Lu, Y.; Yang, L.-M.; Long, N.; Wang, S.-S.; Xie, Z.; Levine, M.; Zou, T.; Sessler, J. L.; Liang, H. Cu(II) complex that synergistically potentiates cytotoxicity and an antitumor immune response by targeting cellular redox homeostasis. *Proc. Natl. Acad. Sci. U. S. A.* **2024**, *121*, No. e2404668121.
(61) Morris, G.; Gevezova, M.; Sarafian, V.; Maes, M. Redox regulation of the immune response. *Cell. Mol. Immunol.* **2022**, *19*, 1079−1101.
(62) Glorieux, C.; Liu, S.; Trachootham, D.; Huang, P. Targeting ROS in cancer: rationale and strategies. *Nat. Rev. Drug Discovery* **2024**, *23*, 583−606.
(63) Alonso-de Castro, S.; Terenzi, A.; Gurruchaga-Pereda, J.; Salassa, L. Catalysis Concepts in Medicinal Inorganic Chemistry. *Chem.—Eur. J.* **2019**, *25*, 6651−6660.
(64) Vucic, S.; Menon, P.; Huynh, W.; Mahoney, C.; Ho, K. S.; Hartford, A.; Rynders, A.; Evan, J.; Evan, J.; Ligozio, S.; Glanzman, R.; Hotchkin, M. T.; Kiernan, M. C. Efficacy and safety of CNM-Au8 in amyotrophic lateral sclerosis (RESCUE-ALS study): A phase 2, randomised, double-blind, placebo-controlled trial and open label extension. *eClinicalMedicine* **2023**, *60*, 102036.
(65) Ren, J.; Dewey, R. B.; Rynders, A.; Evan, J.; Evan, J.; Ligozio, S.; Ho, K. S.; Sguigna, P. V.; Glanzman, R.; Hotchkin, M. T.; Dewey, R. B.; Greenberg, B. M. Evidence of brain target engagement in Parkinson's disease and multiple sclerosis by the investigational nanomedicine, CNM-Au8, in the REPAIR phase 2 clinical trials. *J. Nanobiotechnol.* **2023**, *21*, 478.
(66) Hashmi, A. S. K.; Schäfer, S.; Wölfle, M.; Diez Gil, C.; Fischer, P.; Laguna, A.; Blanco, M. C.; Gimeno, M. C. Gold-Catalyzed Benzylic C−H Activation at Room Temperature. *Angew. Chem., Int. Ed.* **2007**, *46*, 6184−6187.
(67) Sasmal, P. K.; Streu, C. N.; Meggers, E. Metal complex catalysis in living biological systems. *Chem. Commun.* **2013**, *49*, 1581−1587.
(68) Hong, Y.; Lai, Y.-T.; Chan, G. C.-F.; Sun, H. Glutathione and multidrug resistance protein transporter mediate a self-propelled disposal of bismuth in human cells. *Proc. Natl. Acad. Sci. U. S. A.* **2015**, *112*, 3211−3216.
(69) Vidal, C.; Tomás-Gamasa, M.; Destito, P.; López, F.; Mascareñas, J. L. Concurrent and orthogonal gold(I) and ruthenium(II) catalysis inside living cells. *Nat. Commun.* **2018**, *9*, 1913.
(70) Skos, L.; Schmidt, C.; Thomas, S. R.; Park, M.; Geiger, V.; Wenisch, D.; Bonsignore, R.; Del Favero, G.; Mohr, T.; Bileck, A.; Gerner, C.; Casini, A.; Meier-Menches, S. M. Gold-templated covalent targeting of the CysSec-dyad of thioredoxin reductase 1 in cancer cells. *Cell Rep. Phys. Sci.* **2024**, *5*, 102072.
(71) Wu, S.; Wang, X.; He, Y.; Zhu, Z.; Zhu, C.; Guo, Z. A monofunctional trinuclear platinum complex with steric hindrance demonstrates strong cytotoxicity against tumor cells. *J. Inorg. Biochem.* **2014**, *139*, 77−84.
(72) Pérez-López, A. M.; Rubio-Ruiz, B.; Sebastián, V.; Hamilton, L.; Adam, C.; Bray, T. L.; Irusta, S.; Brennan, P. M.; Lloyd-Jones, G. C.; Sieger, D.; Santamaría, J.; Unciti-Broceta, A. Gold-Triggered Uncaging Chemistry in Living Systems. *Angew. Chem., Int. Ed.* **2017**, *56*, 12548−12552.
(73) Tsubokura, K.; Vong, K. K. H.; Pradipta, A. R.; Ogura, A.; Urano, S.; Tahara, T.; Nozaki, S.; Onoe, H.; Nakao, Y.; Sibgatullina, R.; Kurbangalieva, A.; Watanabe, Y.; Tanaka, K. In Vivo Gold Complex Catalysis within Live Mice. *Angew. Chem., Int. Ed.* **2017**, *56*, 3579−3584.
(74) Ebensperger, P.; Zmyslia, M.; Lohner, P.; Braunreuther, J.; Deuringer, B.; Becherer, A.; Süss, R.; Fischer, A.; Jessen-Trefzer, C. A Dual-Metal-Catalyzed Sequential Cascade Reaction in an Engineered Protein Cage. *Angew. Chem., Int. Ed.* **2023**, *62*, No. e202218413.
(75) Dougan, S. J.; Habtemariam, A.; McHale, S. E.; Parsons, S.; Sadler, P. J. Catalytic organometallic anticancer complexes. *Proc. Natl. Acad. Sci. U. S. A.* **2008**, *105*, 11628−33.
(76) Wang, X.; Wang, X.; Jin, S.; Muhammad, N.; Guo, Z. Stimuli-Responsive Therapeutic Metallodrugs. *Chem. Rev.* **2019**, *119*, 1138−1192.
(77) López-Gallego, F.; Salassa, L. Catalysis toward metal-based substrates: A new prospect for inorganic chemistry. *Chem. Catal.* **2023**, *3*, 100459.
(78) López-Hernández, J. E.; Contel, M. Promising heterometallic compounds as anticancer agents: Recent studies in vivo. *Curr. Opin. Chem. Biol.* **2023**, *72*, 102250.
(79) Nguyen, H. D.; Do, L. H. Taming glutathione potentiates metallodrug action. *Curr. Opin. Chem. Biol.* **2022**, *71*, 102213.
(80) Ray, S.; Mohan, R.; Singh, J. K.; Samantaray, M. K.; Shaikh, M. M.; Panda, D.; Ghosh, P. Anticancer and Antimicrobial Metallopharmaceutical Agents Based on Palladium, Gold, and Silver N-Heterocyclic Carbene Complexes. *J. Am. Chem. Soc.* **2007**, *129*, 15042−15053.
(81) Hickey, J. L.; Ruhayel, R. A.; Barnard, P. J.; Baker, M. V.; Berners-Price, S. J.; Filipovska, A. Mitochondria-targeted chemotherapeutics: the rational design of gold(I) N-heterocyclic carbene complexes that are selectively toxic to cancer cells and target protein selenols in preference to thiols. *J. Am. Chem. Soc.* **2008**, *130*, 12570−12571.
(82) Schuh, E.; Pflüger, C.; Citta, A.; Folda, A.; Rigobello, M. P.; Bindoli, A.; Casini, A.; Mohr, F. Gold(I) Carbene Complexes Causing Thioredoxin 1 and Thioredoxin 2 Oxidation as Potential Anticancer Agents. *J. Med. Chem.* **2012**, *55*, 5518−5528.
(83) Hopkinson, M. N.; Richter, C.; Schedler, M.; Glorius, F. An overview of N-heterocyclic carbenes. *Nature* **2014**, *510*, 485−496.
(84) Arambula, J. F.; McCall, R.; Sidoran, K. J.; Magda, D.; Mitchell, N. A.; Bielawski, C. W.; Lynch, V. M.; Sessler, J. L.; Arumugam, K. Targeting antioxidant pathways with ferrocenylated N-heterocyclic carbene supported gold(I) complexes in A549 lung cancer cells. *Chem. Sci.* **2016**, *7*, 1245−1256.
(85) Bazzicalupi, C.; Ferraroni, M.; Papi, F.; Massai, L.; Bertrand, B.; Messori, L.; Gratteri, P.; Casini, A. Determinants for Tight and Selective Binding of a Medicinal Dicarbene Gold(I) Complex to a Telomeric DNA G-Quadruplex: a Joint ESI MS and XRD Investigation. *Angew. Chem., Int. Ed.* **2016**, *55*, 4256−4259.
(86) Liu, W.; Gust, R. Update on metal N-heterocyclic carbene complexes as potential anti-tumor metallodrugs. *Coord. Chem. Rev.* **2016**, *329*, 191−213.
(87) Mora, M.; Gimeno, M. C.; Visbal, R. Recent advances in gold-NHC complexes with biological properties. *Chem. Soc. Rev.* **2019**, *48*, 447−462.

https://doi.org/10.1021/jacs.5c19777
J. Am. Chem. Soc. XXXX, XXX, XXX−XXX

(88) Zhang, C.; Fortin, P.-Y.; Barnoin, G.; Qin, X.; Wang, X.; Fernandez Alvarez, A.; Bijani, C.; Maddelein, M.-L.; Hemmert, C.; Cuvillier, O.; Gornitzka, H. An Artemisinin-Derivative-(NHC)Gold-(I) Hybrid with Enhanced Cytotoxicity through Inhibition of NRF2 Transcriptional Activity. *Angew. Chem., Int. Ed.* **2020**, *59*, 12062−12068.
(89) Herrera, R. P.; Gimeno, M. C. Main Avenues in Gold Coordination Chemistry. *Chem. Rev.* **2021**, *121*, 8311−8363.
(90) Sen, S.; Perrin, M. W.; Sedgwick, A. C.; Lynch, V. M.; Sessler, J. L.; Arambula, J. F. Covalent and non-covalent albumin binding of Au(i) bis-NHCs via post-synthetic amide modification. *Chem. Sci.* **2021**, *12*, 7547−7553.
(91) Wong, K.-H.; Cheung, K.-K.; Chan, M. C.-W.; Che, C.-M. Application of 2,6-Diphenylpyridine as a Tridentate [C∧N∧C] Dianionic Ligand in Organogold(III) Chemistry. Structural and Spectroscopic Properties of Mono- and Binuclear Transmetalated Gold(III) Complexes. *Organometallics* **1998**, *17*, 3505−3511.
(92) Nahra, F.; Tzouras, N. V.; Collado, A.; Nolan, S. P. Synthesis of N-heterocyclic carbene gold(I) complexes. *Nat. Protoc.* **2021**, *16*, 1476−1493.
(93) Karaca, Ö.; Scalcon, V.; Meier-Menches, S. M.; Bonsignore, R.; Brouwer, J. M. J. L.; Tonolo, F.; Folda, A.; Rigobello, M. P.; Kühn, F. E.; Casini, A. Characterization of Hydrophilic Gold(I) N-Heterocyclic Carbene (NHC) Complexes as Potent TrxR Inhibitors Using Biochemical and Mass Spectrometric Approaches. *Inorg. Chem.* **2017**, *56*, 14237−14250.
(94) Schmidt, C.; Albrecht, L.; Balasupramaniam, S.; Misgeld, R.; Karge, B.; Brönstrup, M.; Prokop, A.; Baumann, K.; Reichl, S.; Ott, I. A gold(i) biscarbene complex with improved activity as a TrxR inhibitor and cytotoxic drug: comparative studies with different gold metallodrugs. *Metallomics* **2019**, *11*, 533−545.
(95) Goetzfried, S. K.; Gallati, C. M.; Cziferszky, M.; Talmazan, R. A.; Wurst, K.; Liedl, K. R.; Podewitz, M.; Gust, R. N-Heterocyclic Carbene Gold(I) Complexes: Mechanism of the Ligand Scrambling Reaction and Their Oxidation to Gold(III) in Aqueous Solutions. *Inorg. Chem.* **2020**, *59*, 15312−15323.
(96) Falivene, L.; Cao, Z.; Petta, A.; Serra, L.; Poater, A.; Oliva, R.; Scarano, V.; Cavallo, L. Towards the online computer-aided design of catalytic pockets. *Nat. Chem.* **2019**, *11*, 872−879.
(97) Chang, T.-C.; Vong, K.; Yamamoto, T.; Tanaka, K. Prodrug Activation by Gold Artificial Metalloenzyme-Catalyzed Synthesis of Phenanthridinium Derivatives via Hydroamination. *Angew. Chem., Int. Ed.* **2021**, *60*, 12446−12454.
(98) Mauleon, P.; Toste, F. D. Gold-Catalyzed Reactions of Propargyl Esters, Propargyl Alcohols, and Related Compounds. *Modern Gold Catalyzed Synthesis* **2012**, 75−134.
(99) Tsui, E. Y.; Müller, P.; Sadighi, J. P. Reactions of a Stable Monomeric Gold(I) Hydride Complex. *Angew. Chem., Int. Ed.* **2008**, *47*, 8937−8940.
(100) Liu, Z.; Deeth, R. J.; Butler, J. S.; Habtemariam, A.; Newton, M. E.; Sadler, P. J. Reduction of Quinones by NADH Catalyzed by Organoiridium Complexes. *Angew. Chem., Int. Ed.* **2013**, *52*, 4194−4197.
(101) Liu, Z.; Romero-Canelón, I.; Qamar, B.; Hearn, J. M.; Habtemariam, A.; Barry, N. P. E.; Pizarro, A. M.; Clarkson, G. J.; Sadler, P. J. The potent oxidant anticancer activity of organoiridium catalysts. *Angew. Chem., Int. Ed.* **2014**, *53*, 3941−3946.
(102) Huang, H.; Banerjee, S.; Qiu, K.; Zhang, P.; Blacque, O.; Malcomson, T.; Paterson, M. J.; Clarkson, G. J.; Staniforth, M.; Stavros, V. G.; Gasser, G.; Chao, H.; Sadler, P. J. Targeted photoredox catalysis in cancer cells. *Nat. Chem.* **2019**, *11*, 1041−1048.
(103) Roşca, D.-A.; Fernandez-Cestau, J.; Hughes, D. L.; Bochmann, M. Reactivity of Gold Hydrides: O_2 Insertion into the Au-H Bond. *Organometallics* **2015**, *34*, 2098−2101.
(104) Gaggioli, C. A.; Belpassi, L.; Tarantelli, F.; Zuccaccia, D.; Harvey, J. N.; Belanzoni, P. Dioxygen insertion into the gold(i)-hydride bond: spin orbit coupling effects in the spotlight for oxidative addition. *Chem. Sci.* **2016**, *7*, 7034−7039.
(105) Phearman, A. S.; Ardon, Y.; Goldberg, K. I. Insertion of Molecular Oxygen into a Gold(III)-Hydride Bond. *J. Am. Chem. Soc.* **2024**, *146*, 4045−4059.
(106) Betanzos-Lara, S.; Liu, Z.; Habtemariam, A.; Pizarro, A. M.; Qamar, B.; Sadler, P. J. Organometallic Ruthenium and Iridium Transfer-Hydrogenation Catalysts Using Coenzyme NADH as a Cofactor. *Angew. Chem., Int. Ed.* **2012**, *51*, 3897−3900.
(107) Bose, S.; Ngo, A. H.; Do, L. H. Intracellular Transfer Hydrogenation Mediated by Unprotected Organoiridium Catalysts. *J. Am. Chem. Soc.* **2017**, *139*, 8792−8795.
(108) Coverdale, J. P. C.; Romero-Canelón, I.; Sanchez-Cano, C.; Clarkson, G. J.; Habtemariam, A.; Wills, M.; Sadler, P. J. Asymmetric transfer hydrogenation by synthetic catalysts in cancer cells. *Nat. Chem.* **2018**, *10*, 347.
(109) Weng, C.; Shen, L.; Teo, J. W.; Lim, Z. C.; Loh, B. S.; Ang, W. H. Targeted Antibacterial Strategy Based on Reactive Oxygen Species Generated from Dioxygen Reduction Using an Organoruthenium Complex. *JACS Au* **2021**, *1*, 1348−1354.
(110) Weng, C.; Yang, H.; Loh, B. S.; Wong, M. W.; Ang, W. H. Targeting Pathogenic Formate-Dependent Bacteria with a Bioinspired Metallo-Nitroreductase Complex. *J. Am. Chem. Soc.* **2023**, *145*, 6453−6461.
(111) Móran Plata, M. J.; Marretta, L.; Gaztelumendi, L.; Pieslinger, G. E.; Carballo, R. R.; Rezabal, E.; Barone, G.; Martínez-Martínez, V.; Terenzi, A.; Salassa, L. Alloxazine-Based Ligands and Their Ruthenium Complexes as NADH Oxidation Catalysts and G4 Binders. *Inorg. Chem.* **2024**, *63*, 16362−16373.
(112) Regeni, I.; Bonnet, S. Supramolecular approaches for the treatment of hypoxic regions in tumours. *Nat. Rev. Chem.* **2025**, *9*, 365−377.
(113) Jana, R. D.; Nguyen, H. D.; Do, L. H. Selective Iridium-Catalyzed Reductive Amination Inside Living Cells. *J. Am. Chem. Soc.* **2025**, *147*, 23318−23330.
(114) Vong, K.; Yamamoto, T.; Chang, T.-c.; Tanaka, K. Bioorthogonal release of anticancer drugs via gold-triggered 2-alkynylbenzamide cyclization. *Chem. Sci.* **2020**, *11*, 10928−10933.
(115) Vitali, V.; Massai, L.; Messori, L. Strategies for the design of analogs of auranofin endowed with anticancer potential. *Expert Opin. Drug Discovery* **2024**, *19*, 855−867.
(116) Zou, T.; Lum, C. T.; Chui, S. S.-Y.; Che, C.-M. Gold(III) Complexes Containing N-Heterocyclic Carbene Ligands: Thiol "Switch-on" Fluorescent Probes and Anti-Cancer Agents. *Angew. Chem., Int. Ed.* **2013**, *52*, 2930−2933.
(117) Sykes, S. M.; Di Marcantonio, D.; Martinez, E.; Huhn, J.; Gupta, A.; Mistry, R. JUN and ATF3 Regulate the Transcriptional Output of the Unfolded Protein Response to Support Acute Myeloid Leukemia. *Blood* **2018**, *132*, 1327.
(118) Hoetzenecker, W.; Echtenacher, B.; Guenova, E.; Hoetzenecker, K.; Woelbing, F.; Brück, J.; Teske, A.; Valtcheva, N.; Fuchs, K.; Kneilling, M.; Park, J.-H.; Kim, K.-H.; Kim, K.-W.; Hoffmann, P.; Krenn, C.; Hai, T.; Ghoreschi, K.; Biedermann, T.; Röcken, M. ROS-induced ATF3 causes susceptibility to secondary infections during sepsis-associated immunosuppression. *Nat. Med.* **2012**, *18*, 128−134.
(119) Mitchell, D. C.; Kuljanin, M.; Li, J.; Van Vranken, J. G.; Bulloch, N.; Schweppe, D. K.; Huttlin, E. L.; Gygi, S. P. A proteome-wide atlas of drug mechanism of action. *Nat. Biotechnol.* **2023**, *41*, 845−857.
(120) Li, H. Y.; Zhang, J.; Sun, L. L.; Li, B. H.; Gao, H. L.; Xie, T.; Zhang, N.; Ye, Z. M. Celastrol induces apoptosis and autophagy via the ROS/JNK signaling pathway in human osteosarcoma cells: an in vitro and in vivo study. *Cell Death Dis.* **2015**, *6*, No. e1604.
(121) Liu, X.; Zhao, P.; Wang, X.; Wang, L.; Zhu, Y.; Song, Y.; Gao, W. Celastrol mediates autophagy and apoptosis via the ROS/JNK and Akt/mTOR signaling pathways in glioma cells. *J. Exp. Clin. Cancer Res.* **2019**, *38*, 184.
(122) Chen, X.; Zhao, Y.; Luo, W.; Chen, S.; Lin, F.; Zhang, X.; Fan, S.; Shen, X.; Wang, Y.; Liang, G. Celastrol induces ROS-mediated

https://doi.org/10.1021/jacs.5c19777
J. Am. Chem. Soc. XXXX, XXX, XXX−XXX

apoptosis via directly targeting peroxiredoxin-2 in gastric cancer cells. *Theranostics* **2020**, *10*, 10290−10308.
(123) Szklarczyk, D.; Kirsch, R.; Koutrouli, M.; Nastou, K.; Mehryary, F.; Hachilif, R.; Gable, A. L; Fang, T.; Doncheva, N. T; Pyysalo, S.; Bork, P.; Jensen, L. J; von Mering, C. The STRING database in 2023: protein-protein association networks and functional enrichment analyses for any sequenced genome of interest. *Nucleic Acids Res.* **2023**, *51*, D638−D646.
(124) Omata, Y.; Folan, M.; Shaw, M.; Messer, R. L.; Lockwood, P. E.; Hobbs, D.; Bouillaguet, S.; Sano, H.; Lewis, J. B.; Wataha, J. C. Sublethal concentrations of diverse gold compounds inhibit mammalian cytosolic thioredoxin reductase (TrxR1). *Toxicol. in Vitro* **2006**, *20*, 882−890.
(125) Saei, A. A.; Gullberg, H.; Sabatier, P.; Beusch, C. M.; Johansson, K.; Lundgren, B.; Arvidsson, P. I.; Arnér, E. S. J.; Zubarev, R. A. Comprehensive chemical proteomics for target deconvolution of the redox active drug auranofin. *Redox Biol.* **2020**, *32*, 101491.
(126) Li, X.; Zhang, B.; Yan, C.; Li, J.; Wang, S.; Wei, X.; Jiang, X.; Zhou, P.; Fang, J. A fast and specific fluorescent probe for thioredoxin reductase that works via disulphide bond cleavage. *Nat. Commun.* **2019**, *10*, 2745.
(127) Chiappetta, G.; Gamberi, T.; Faienza, F.; Limaj, X.; Rizza, S.; Messori, L.; Filomeni, G.; Modesti, A.; Vinh, J. Redox proteome analysis of auranofin exposed ovarian cancer cells (A2780). *Redox Biol.* **2022**, *52*, 102294.
(128) Sen Santara, S.; Lee, D.-J.; Crespo, Â.; Hu, J. J.; Walker, C.; Ma, X.; Zhang, Y.; Chowdhury, S.; Meza-Sosa, K. F.; Lewandrowski, M.; Zhang, H.; Rowe, M.; McClelland, A.; Wu, H.; Junqueira, C.; Lieberman, J. The NK cell receptor NKp46 recognizes ecto-calreticulin on ER-stressed cells. *Nature* **2023**, *616*, 348−356.
(129) Guilbaud, E.; Kroemer, G.; Galluzzi, L. Calreticulin exposure orchestrates innate immunosurveillance. *Cancer Cell* **2023**, *41*, 1014−1016.
(130) Obeid, M.; Tesniere, A.; Ghiringhelli, F.; Fimia, G. M.; Apetoh, L.; Perfettini, J.-L.; Castedo, M.; Mignot, G.; Panaretakis, T.; Casares, N.; Métivier, D.; Larochette, N.; van Endert, P.; Ciccosanti, F.; Piacentini, M.; Zitvogel, L.; Kroemer, G. Calreticulin exposure dictates the immunogenicity of cancer cell death. *Nat. Med.* **2007**, *13*, 54−61.
(131) Leavy, O. Regulating ROS. *Nat. Rev. Immunol.* **2014**, *14*, 357−357.
(132) Bettelli, E.; Carrier, Y.; Gao, W.; Korn, T.; Strom, T. B.; Oukka, M.; Weiner, H. L.; Kuchroo, V. K. Reciprocal developmental pathways for the generation of pathogenic effector TH17 and regulatory T cells. *Nature* **2006**, *441*, 235−238.

https://doi.org/10.1021/jacs.5c19777
J. Am. Chem. Soc. XXXX, XXX, XXX−XXX